Int. J. Heat Mass Transfer. Vol. 32, No. 7, pp. 1383–1386, 1989
Printed in Great Britain

0017-9310/89 $3.00+0.00

Analysis of heat and momentum transport along a moving surface

P. R. CHAPPIDI and F. S. GUNNERSON

College of Engineering, University of Central Florida, P.O. Box 25000, Orlando, FL 32816, U.S.A.

(*Received* 4 *May* 1988 *and in final form* 3 *January* 1989)

INTRODUCTION

IN CERTAIN metal and polymer forming processes such as extrusion, hot rolling and drawing, a hot flat sheet or a cylindrical rod issues continuously from a slot or die and exchanges heat with the surrounding fluid medium on route to the take-up reel (Fig. 1). Information regarding the momentum exchange and heat transfer along such a moving surface may be useful in determining the heat transfer rates in manufacturing processes.

In view of these applications, Sakiadis [1] presented theoretical solutions for a flat surface moving in a quiescent fluid. Tsou *et al.* [2] showed that this flow is physically realizable under laboratory conditions and theoretically analyzed the stability of the flow [4]. Later investigations addressed the influence of variable fluid properties [4], buoyancy [5] and transverse conduction effects within the moving surface [6]. These analyses pertain to a special case ($u_\infty = 0$) of the more general analysis where the surface and the ambient free stream fluid are in motion. Abdelhafez [7] recently presented a numerical analysis of the general problem, including a solution of the corresponding Navier–Stokes equations.

In this note, flow and thermal transport from a surface moving through a flowing fluid are investigated both analytically and numerically. By using an integral technique along with a perturbation procedure, simple closed form expressions are obtained in this study as a function of the velocity differential between the surface and the free stream fluid. The resulting expressions permit quick estimations of the skin friction and heat transfer rates thereby circumventing the computer calculations used in previous studies. Comparisons with the numerical simulations indicate the analytical expressions to be fairly accurate.

ANALYSIS

Consider a solid flat surface of temperature T_w issuing from a slot at a constant velocity u_w (Fig. 1). For a steady, laminar, two-dimensional and incompressible flow with uniform wall temperature conditions, the governing boundary layer equations (mass, momentum and energy) as developed by Sakiadis [1] (with the boundary conditions, at $y = 0$: $u = u_w$, $t = t_w$ and at $y = \delta$, δ_t: $u = u_\infty$, $t = t_\infty$) apply. Boundary layer assumptions are not satisfied near the slot wall due to edge influences. Axial conduction within the flat surface also invalidates the boundary layer assumptions. Far away from the entrance slot, the influence of edge effects is minimal. For a high Peclet number flow, the axial conduction within the surface can be neglected. Thus, the results of this boundary layer analysis with isothermal wall conditions may be applicable to a thin flat surface, away from the entrance slot in a high Peclet number flow. The integral form of the governing equations is obtained after integration from $y = 0$ to δ, δ_t as

$$\frac{\mathrm{d}}{\mathrm{d}x}\left\{\delta\int_0^1 \frac{u}{u_i}\left(\frac{u}{u_i}-\frac{u_\infty}{u_i}\right)\mathrm{d}\eta\right\} = \frac{-\tau_w}{\rho u_i^2} \tag{1}$$

$$\frac{\mathrm{d}}{\mathrm{d}x}\left\{\delta_t\int_0^1 \frac{u}{u_i}\left(\frac{t-t_\infty}{t_w-t_\infty}\right)\mathrm{d}\xi\right\} = \frac{q_w}{\rho C_p u_i (t_w-t_\infty)} \tag{2}$$

where

$$\text{for } u_w \geqslant u_\infty, \quad i = \mathrm{w}$$
$$\text{for } u_w \leqslant u_\infty, \quad i = \infty.$$

The boundary conditions are

at $y = 0$:

$$u = u_w, \quad \frac{\partial^2 u}{\partial y^2} = 0, \quad t = t_w, \quad \frac{\partial^2 t}{\partial y^2} = 0 \tag{3}$$

at $y = \delta$:

$$u = u_\infty, \quad \frac{\partial u}{\partial y} = \frac{\partial^2 u}{\partial y^2} = 0 \tag{4}$$

at $y = \delta_t$:

$$t = t_\infty, \quad \frac{\partial t}{\partial y} = \frac{\partial^2 t}{\partial y^2} = 0 \tag{5}$$

where

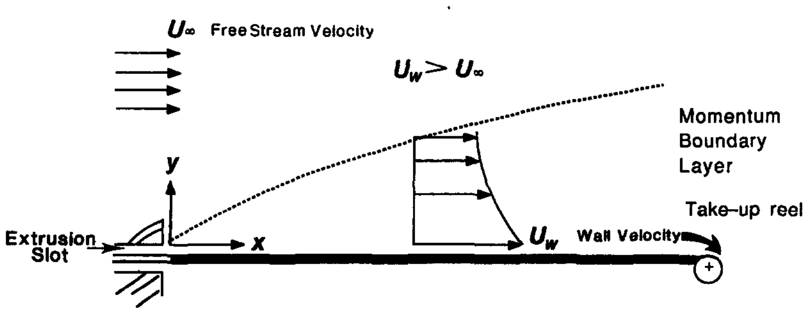

FIG. 1. Flow model of a moving surface.

NOMENCLATURE

C_{fx}	local skin friction coefficient defined by equations (10) and (18)
C_p	specific heat of the fluid
h_x	local heat transfer coefficient
k	thermal conductivity of the fluid
L	characteristic length of the surface
Nu_x	local Nusselt number defined by equations (16) or (21)
Pe	Peclet number, $u_t L/\alpha_s$
Pr	Prandtl number of the fluid
q	local heat flux
R	velocity differential parameter, equations (9) and (17)
Re_x	local Reynolds number
t	temperature
u,v	streamwise and transverse components of velocity.

Greek symbols

α_s	thermal diffusivity of the solid
δ,δ_t	thickness of the velocity and thermal boundary layers
η	non-dimensional thickness, y/δ
μ	absolute viscosity
ν	kinematic viscosity
ξ	non-dimensional thickness, y/δ_t
ρ	density
τ	shear stress.

Subscripts

w	wall
∞	free stream.

$$\tau_w = \mu\left(\frac{\partial u}{\partial y}\right)_{y=0}, \quad q_w = -k\left(\frac{\partial t}{\partial y}\right)_{y=0}. \tag{6}$$

Fourth-order velocity and temperature profiles satisfying the above boundary conditions are chosen, namely

$$\frac{u}{u_t} = \frac{u_w}{u_t} + \left(1-\frac{u_w}{u_\infty}\right)(2\eta - 2\eta^3 + \eta^4) \tag{7}$$

$$\frac{t-t_\infty}{t_w - t_\infty} = 1 - 2\xi + 2\xi^3 - \xi^4. \tag{8}$$

Case 1 : $u_w \geqslant u_\infty$

Solution of the momentum equation (1) with the velocity profile (7) and the boundary condition $\delta(x=0) = 0$ yields

$$\frac{\delta}{x} Re_x^{1/2} = 2\left(\frac{R}{0.3R - 0.1174R^2}\right)^{1/2}$$

where

$$R = 1 - \frac{u_\infty}{u_w}, \quad Re_x = \frac{u_w x}{\nu}. \tag{9}$$

The local skin coefficient is defined as

$$C_{fx} = \frac{\mu\left(\frac{\partial u}{\partial y}\right)_{y=0}}{\frac{1}{2}\rho u_w^2} = \frac{2(R(0.3R-0.1174R^2))^{1/2}}{Re_x^{1/2}}. \tag{10}$$

Substituting the velocity and temperature profiles, equations (7) and (8), into the energy equation (2) and integrating for fluids with $Pr \geqslant 1$ yields

$$\Delta\delta\frac{d}{dx}\left(\delta\left(\frac{3}{10}\Delta - \frac{2}{15}R\Delta^2 + \frac{3}{140}R\Delta^4 - \frac{1}{80}R\Delta^6\right)\right) = \frac{2k}{\rho C_p u_w},$$

$$\Delta = \frac{\delta_t}{\delta}. \tag{11}$$

To solve the above non-linear differential equation, a perturbation series of the type

$$\Delta = \sum_{n=0}^{\infty} R^n \Delta_n$$

is assumed, substituted in equation (11) and coefficients of like powers of R compared. This yields (note: for simplicity attention is restricted to the first two powers R^0, R^1)

$$R^0 : \Delta_0 \delta \frac{d}{dx}\left(\frac{3}{10}\Delta_0\delta\right) = \frac{2k}{\rho C_p u_w} \tag{12}$$

$$R^1 : \frac{3}{10}\delta\left(\Delta_0 \frac{d}{dx}(\Delta_1\delta) + \Delta_1\frac{d}{dx}(\Delta_0\delta)\right) - \frac{2}{15}\Delta_0\delta\frac{d}{dx}(\Delta_0^2\delta) = 0. \tag{13}$$

Solving the above equations yield

$$\Delta_0 = \left(\frac{10}{3PrA_1}\right)^{1/2}, \quad \Delta_1 = \frac{20}{27(PrA_1)^{1/2}}$$

where

$$A_1 = \frac{R}{(0.3R - 0.1174R^2)}. \tag{14}$$

A two-term approximation of the above series $\Delta \cong \Delta_0 + R\Delta_1$ yields

$$\frac{\delta_t}{x}(Re_x)^{1/2} = \frac{2}{Pr^{1/2}}\left\{\left(\frac{10}{3}\right)^{1/2} + R\left(\frac{20}{27(PrA_1)^{1/2}}\right)\right\} \tag{15}$$

$$Nu_x = \frac{hx}{k} = \frac{q_w x}{(t_w - t_\infty)k} = \frac{Re_x^{1/2}\,Pr^{1/2}}{\left(\left(\frac{10}{3}\right)^{1/2} + \frac{20R}{27(PrA_1)^{1/2}}\right)}. \tag{16}$$

Case 2 : $u_w \leqslant u_\infty$

The analysis is similar to the earlier case. Equations (7) and (8) are substituted into equations (1) and (2) and integrated to obtain

$$\frac{\delta}{x}Re_x^{1/2} = 2\left(\frac{R}{(0.3R - 0.1824R^2)}\right)^{1/2}, \quad R = 1 - \frac{u_w}{u_\infty},$$

$$Re_x = \frac{u_\infty x}{\nu}. \tag{17}$$

The local skin friction coefficient is defined as

$$C_{fx} = \frac{\mu\left(\frac{\partial u}{\partial y}\right)_{y=0}}{\frac{1}{2}\rho u_\infty^2} = \frac{2\{R(0.3R-0.1824R^2)\}^{1/2}}{Re_x^{1/2}}. \tag{18}$$

Further, the integral energy equation (2) yields

$$\Delta \cong \Delta_0 + R\Delta_1 = \left\{\frac{10}{(3PrA_1)}\right\}^{1/2} + \left\{\frac{RA_2}{(A_1 Pr)^{1/2}}\right\}$$

where

$$A_2 = \left(\frac{5}{6}\right)^{1/2} - \left\{\frac{40}{54(PrA_1)^{1/2}}\right\}. \tag{19}$$

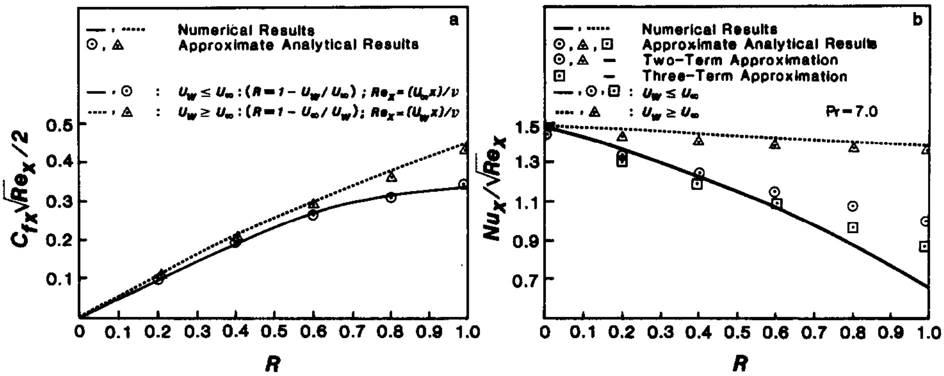

FIG. 2. Skin friction and wall heat transfer results as a function of the velocity differential parameter R ($Pr \cong 7.0$).

Thus, the thermal boundary layer thickness is

$$\frac{\delta_t}{x} Re_x^{1/2} = \frac{2\left(\left(\frac{10}{3}\right)^{1/2} + RA_2\right)}{Pr^{1/2}}. \tag{20}$$

Hence the Nusselt number is

$$Nu_x = \frac{hx}{k} = \frac{q_w x}{(t_w - t_\infty)k} = \frac{Re_x^{1/2}\, Pr^{1/2}}{\left(\left(\frac{10}{3}\right)^{1/2} + RA_2\right)}. \tag{21}$$

In order to compare the results of the approximate expressions derived (equations (10), (16), (18) and (21)), numerical solutions were obtained for water ($Pr = 7$) and air ($Pr = 0.7$). Governing equations were considered in the similarity form [7] and a fourth-order Runge–Kutta method [8] was used to obtain the solution of the velocity field. The temperature profiles were obtained by solving the energy equation in an implicit finite difference form. A step size of 0.025, $\eta_{maximum} = 10$ and a convergence criterion of 10^{-6} (to satisfy the free stream velocity boundary condition) were used in the numerical simulations.

RESULTS

Figure 2 shows the dependence of skin friction ($C_{fx} Re_x^{1/2}/2$) and heat transfer ($Nu_x/Re_x^{1/2}$) as a function of the velocity differential R between the solid surface and the flowing free stream. The skin friction results, equations (10) and (18), compare to within 4% of the numerical solutions. For the case $u_w \geqslant u_\infty$, the analytical heat transfer results compare within 3% to the numerical results. When $u_w \leqslant u_\infty$, as R increases beyond 0.5 (Fig. 2(b)), heat transfer results obtained by the two-term approximation begin to diverge considerably from the numerical solution. As $R \to 1$, the difference is as much as 53% for water. In order to obtain more accuracy, a three-term approximate series of Δ was considered. This yields

$$\frac{Nu_x}{Re_x^{1/2}} = \frac{Pr^{1/2}}{\left(\frac{10}{3}\right)^{1/2} + RA_2 + R^2 A_3} \tag{22}$$

where

$$A_3 = A_2 - A_2\left(\frac{640}{243RA_1}\right)^{1/2} - A_2^2\left(\frac{Pr\,A_1}{400}\right)^{1/2}. \tag{23}$$

The difference ($Pr = 7$, $R \to 1$) reduced to 34%. An extension of the current analysis to air ($Pr \cong 0.7$) yields the results given in Table 1. Further inspection of Fig. 2 reveals that the analytical skin friction predictions are closer to the numerical results as compared to the heat transfer predictions. This could probably be attributed to the additional approximations (i.e. truncation of the series of Δ, linearization of the non-linear differential equation by the series technique) used in solving the energy equation.

The skin friction and heat transfer results of a surface moving faster than the free stream ($u_w > u_\infty$) are higher as compared to a surface moving slower than the free stream ($u_w < u_\infty$) (Fig. 2). The reason is, for the same velocity differential (R) and the same Reynolds number (Re_x), the momentum and thermal boundary layers (δ, δ_t) are thinner in the former case, $u_w > u_\infty$ as opposed to the latter case, $u_w < u_\infty$ (see equations (9), (15), (17) and (20)). For thinner shear and thermal boundary layers, sharper gradients exist at the wall leading to higher skin friction and heat transfer

Table 1. Comparison of Nusselt numbers for air ($Pr = 0.7$)

		$U_w \geqslant U_\infty$			$U_w \leqslant U_\infty$	
R		$Nu_x/\sqrt{(Re_x)}$	%D		$Nu_x/\sqrt{(Re_x)}$	%D
0	N	0.47	−2	N	0.47	
	$A2$	0.4583		$A2$	0.4583	−2
				$A3$	0.4583	−2
0.2	N	0.453	−4	N	0.4445	
	$A2$	0.436		$A2$	0.4362	−2
				$A3$	0.4362	−2
0.4	N	0.4315	−3	N	0.4134	
	$A2$	0.4175		$A2$	0.4137	≃0
				$A3$	0.4132	≃0
0.6	N	0.4085	−2	N	0.3789	
	$A2$	0.4022		$A2$	0.3907	3
				$A3$	0.3872	2
0.8	N	0.3823	2	N	0.3401	
	$A2$	0.3896		$A2$	0.3673	8
				$A3$	0.3572	5
1.0	N	0.3525	8	N	0.294	
	$A2$	0.3976		$A2$	0.3436	17
				$A3$	0.3226	10

N, numerical solution of Abdelhafez [7]; $A2$, two-term series solution; $A3$, three-term series solution; %D, difference, $((N - A2 \text{ or } A3)/N) \times 100$.

rates. The decreasing trend of the skin friction (Fig. 2(a)) as $R \to 0$ is due to the reduction in the relative velocity between the plate and the free stream. This leads to milder velocity gradients at the wall decreasing the skin friction. As R decreases, the heat transfer parameter $(Nu_x/Re_x^{1/2})$ increases (Fig. 2). Since the velocity field drives the temperature field in forced convection, increased fluid velocities near the wall (a result of a decrease in R) enhance the heat transfer.

CONCLUSIONS

Analytical expressions were developed to estimate the skin friction and heat transfer for a surface moving in a flowing fluid. Analytical predictions match the numerical simulations to within 4% for skin friction. Heat transfer predictions likewise compare well (maximum deviation is about 8%) with the numerical results when $u_w > u_\infty$; $0 < R \leqslant 1$. For $u_w < u_\infty$ (as $R \to 1$) the error committed by using the approximate relations can increase up to 35% for water ($Pr = 7$) and 10% for air ($Pr = 0.7$). Current expressions permit quick estimations of the skin friction and heat transfer circumventing the need for computer calculations. Since boundary layer approximations are made with isothermal wall conditions, they may be valid only for a thin flat surface away from the entrance slot, in a high Peclet number flow.

REFERENCES

1. B. C. Sakiadis, Boundary-layer behavior on continuous solid surface—parts 1 and 2, *A.I.Ch.E. Jl* **7**, 26–28, 221–225 (1961).
2. F. Tsou, E. M. Sparrow and R. Goldstein, Flow and heat transfer in the boundary layer on a continuous moving surface, *Int. J. Heat Mass Transfer* **10**, 219–235 (1967).
3. F. Tsou, E. M. Sparrow and E. F. Kurtz, Hydrodynamic stability of the boundary layer on a continuous moving surface, *J. Fluid Mech.* **26**, 145–161 (1966).
4. I. G. Choi, The effect of variable properties of air on the boundary layer for a moving continuous cylinder, *Int. J. Heat Mass Transfer* **25**, 597–602 (1982).
5. A. Moutsoglou and A. K. Bhattacharya, Laminar and turbulent boundary layers on moving, non-isothermal continuous surfaces, *J. Heat Transfer* **104**, 707–714 (1982).
6. M. Karwe and Y. Jaluria, Thermal transport from a heated moving surface, *J. Heat Transfer* **108**, 728–734 (1986).
7. T. A. Abdelhafez, Skin friction and heat transfer on a continuous flat surface moving in a parallel free stream, *Int. J. Heat Mass Transfer* **28**, 1234–1237 (1985).
8. C. Y. Chow, *An Introduction to Computational Fluid Mechanics* (Corrected Edn). Seminole, Boulder, Colorado (1983).